World Scientific
www.worldscientific.com

NOISE-INDUCED PHASE SYNCHRONIZATION AMONG ANALOG MOS OSCILLATOR CIRCUITS

AKIRA UTAGAWA, TETSUYA ASAI*
and YOSHIHITO AMEMIYA

*Graduate School of Information Science and Technology
Hokkaido University, Kita 14, Nishi 9
Kita-ku, Sapporo, 060-0814, Japan
asai@ist.hokudai.ac.jp

In this paper, we experimentally demonstrate noise-induced phase synchronization among multiple electrical oscillator circuits constructed by discrete MOS devices, where multiple nonlinear oscillators can be synchronized with each other when they accept common pulse perturbations randomly distributed in time. We also show that nonidentical oscillator circuits have the same peak frequency in a power spectrum when they receive a common perturbation.

Keywords: Noise-induced phase synchronization; nonlinear oscillator; analog MOS circuits; Wilson–Cowan system.

1. Introduction

Synchronization among nonlinear oscillators can be observed everywhere in the world, and has attracted much attention from many scientific and engineering fields. Noise-induced synchronization among nonlinear oscillators has been one of the topic of great relevance and long-standing controversy (e.g., [1–6]), where individual nonlinear oscillators can be synchronized by applying common random noises to the oscillators. This implies that when one considers embedding multiple oscillators on hardware, phases of the oscillators could be synchronized by applying common random noises, and the oscillators distributed on the hardware (e.g., large-scale integrated circuits) can be utilized as synchronized "clock sources".

Inspired by the results and implications above, we previously proposed hardware oscillator circuits based on Wilson–Cowan oscillator model [7] that is suitable for hardware implementation, and showed that synchronization properties of the Wilson–Cowan model were qualitatively equivalent to those of the conventional model [8]. Through circuit simulations, we demonstrated noise-induced

synchronization among the hardware oscillators, and evaluated the synchrony dependence on device mismatches between two oscillator circuits. The result showed that: (i) the oscillators exhibited phase-locked oscillation and (ii) the circuit had small tolerance on device mismatches, although small phase difference exist [8].

Because our previous results on noise-induced synchronization among Wilson–Cowan oscillator circuits were obtained from computer simulations only, in this paper we show experimental results of noise-induced phase synchronization among nonlinear oscillator circuits by using discrete MOS devices, and evaluate the effects of device mismatches in the oscillators on phase synchronization. The results may ensure that noise-induced phase synchronization occurs in real world under a certain range of nonidentical conditions.

2. Phase Synchronization Among Noise-Driven Wilson–Cowan Oscillators

We here employ a noise-driven Wilson–Cowan oscillator [7] to demonstrate noise-induced synchronization among hardware oscillators. Its dynamics are given by

$$\dot{u}_i = -u_i + f_\beta(u_i - v_i) + \alpha I(t), \tag{1}$$

$$\dot{v}_i = -v_i + f_\beta(u_i - \theta), \tag{2}$$

where u_i and v_i represent the system variables of the ith oscillator, θ the threshold, $I(t)$ the common random impulses ($\in 0, 1$), α the strength of the impulses and $f_\beta(\cdot)$ the sigmoid function with slope β.

Figures 1 and 2 show numerical examples of a noise-driven Wilson–Cowan oscillator receiving random impulses given by

$$I(t) = \alpha \left\{ \sum_j \delta(t - t_j^{(1)}) - \delta(t - t_j^{(2)}) \right\}, \tag{3}$$

where $\delta(t) = \Theta(t) - \Theta(t - w)$ (Θ, w and t_j represent the step function, the pulse width and the positive random number with $t_j^{(1)} \neq t_j^{(2)}$ for all js, respectively). In Figs. 1 and 2, system parameters were set at $\theta = 0.5$, $\beta = 10$, $\alpha = 0.5$, $w = 0.1$, and the averaged inter-spike interval of $|I(t)|$ was set at 100. Transient waveforms of u_i and v_i were fluctuated by $I(t)$, as shown in Fig. 1. Figure 2 shows trajectories and nullclines on a phase ($u_i - v_i$) plane, exhibiting that the trajectory was clearly fluctuated by $I(t)$.

To demonstrate noise-induced synchronization among the oscillators, we employ multiple Wilson–Cowan oscillators. Let us assume that all the oscillators have the same system parameters, and accept (or do not accept) the common random impulses $I(t)$. Figure 3 shows examples of raster plots extracted from transient waveforms of the oscillators with $N = 10$ (N: the number of oscillators) where vertical bars were plotted at which $u_i > 0.5$ and $du_i/dt > 0$ ($i = 1 \sim 10$). In this example, the initial condition of each oscillator was randomly chosen. When the
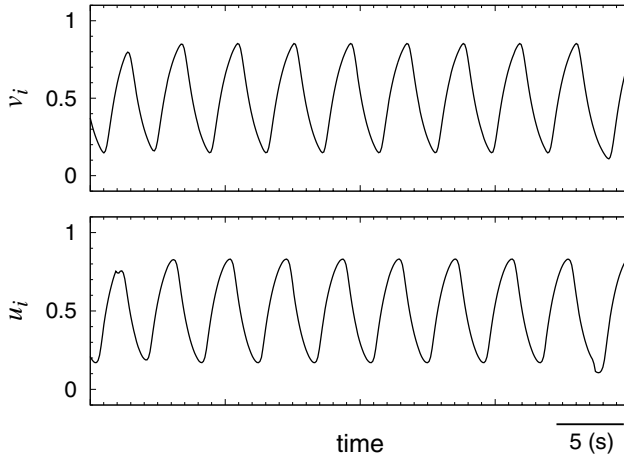
Fig. 1. Time courses of system variables of single Wilson–Cowan oscillator receiving common random impulses.
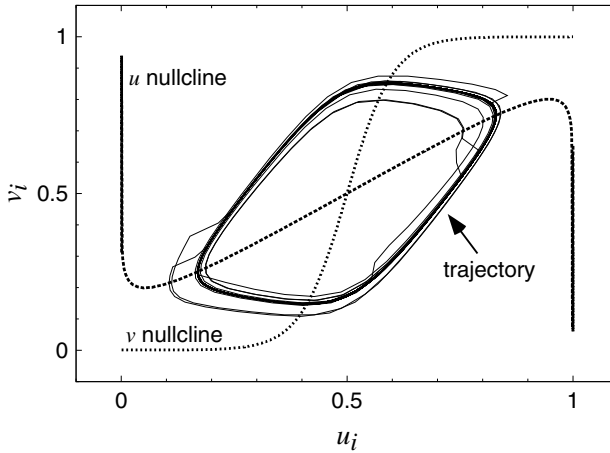

Fig. 2. Nullclines and trajectories of single Wilson–Cowan oscillator receiving common random impulses.

oscillators did not accept $I(t)$ ($\alpha = 0$), they exhibited independent oscillations as shown in Fig. 3(a). In contrast, all the oscillators were synchronized when they accepted noises ($\alpha = 0.5$), as shown in Fig. 3(b). To evaluate the degree of the synchronization, we employ the following order parameter:

$$R(t) = \frac{1}{N} \left| \sum_j \exp(i\phi_j) \right|,$$
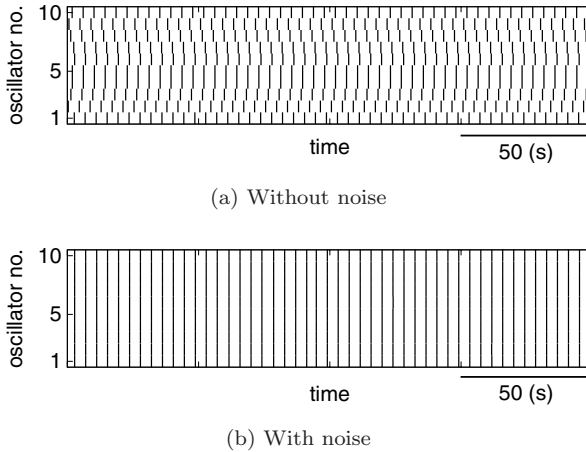
(a) Without noise

(b) With noise

Fig. 3. Raster plots of 10 oscillators: (a) independent oscillations without common random impulses and (b) synchronous oscillations with common random impulses.

where i is the imaginary unit [9]. When all the oscillators are synchronized, $R(t)$ becomes equal to 1 because of the uniform ϕ_js, while $R(t)$ is less than 1 if the oscillators are not synchronized. Figure 4 shows the time courses of the order parameter values. When $\alpha = 0$, $R(t)$ was unstable and was always less than 1 [Fig. 4(a)], whereas $R(t)$ remained at 1 after it became stable at $t \approx 5000$ when $\alpha = 0.5$ [Fig. 4(b)]. These examples above demonstrated that a set of noise-driven Wilson–Cowan oscillators with different initial conditions exhibited noise-induced synchronization when they received common random impulses, although a different type of oscillators (non-FitzHugh–Nagumo oscillators) was employed.
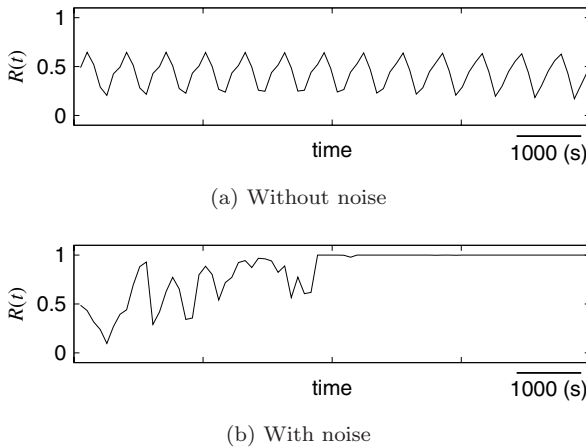

(a) Without noise

(b) With noise

Fig. 4. Time courses of order parameter values: (a) without common random impulses and (b) with common random impulses.

3. A Noise-Driven MOS Oscillator Circuit

Figure 5 shows a schematic of a MOS oscillator circuit based on the Wilson–Cowan model [8, 10, 11]. The circuit consists of a MOS transconductance amplifier, a buffer circuit consisting of two standard inverters, and two capacitors (C_1 and C_2). Since output u_i of the transconductance amplifier is fed back to its positive input V_p, when negative input voltage V_m ($= v_i$) of the amplifier is increased from 0 to V_{dd}, u_i is inverted (from V_{dd} to 0) at a higher threshold voltage (around V_{dd}). When V_m is decreased from V_{dd} to 0, u_i is inverted (from 0 to V_{dd}) at a lower threshold voltage (around 0). Therefore, this "positive-feedback" amplifier exhibits large hysteresis in the v_i–u_i characteristic [10], and acts as a Schmitt trigger-like inverter. Since the output of the amplifier (u_i) is fed to two inverters (a buffer circuit) and the output of the buffer (v_i) is fed back to the input of the amplifier (V_m), the overall circuit construction is similar to a ring oscillator consisting of three inverting amplifiers (one Schmitt trigger inverter and two standard inverter).

The oscillation frequency can be controlled by the supply voltage and the capacitances (C_1 and C_2), as in standard ring oscillators. The oscillation frequency also depends on V_n since response frequencies of a MOS transconductance amplifier is mainly determined by the tail current of the amplifier. Because the tail current increases vastly as V_n increases, small fluctuation in V_n may fluctuate the oscillator circuit effectively. We here employ a standard M-sequence circuit [12] as a noise source that generates 0–1 random streams. By differentiating the output of the M-sequence circuit (V_{mseq}), one can obtain impulsive random sequences. To do this, a differentiator (C_0 and r_0) is employed, as shown in Fig. 5. The random impulsive voltage is generated at V_n where the DC bias voltage is set by V_{bias} and the decay time is given by $C_0 r_0$. Note that in our experiments the oscillator's intrinsic frequency is tuned by V_{bias}, and the strength of the impulsive noise is controlled by C_0.
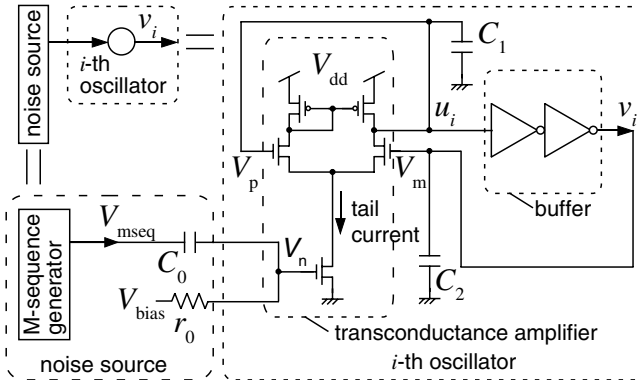

Fig. 5. Noise-driven MOS oscillator circuit.

4. Measurement Results

In the following experiments, we employed discrete electrical devices ($C_0 = 21\,\mathrm{pF}$, $C_1 = 4.7\,\mathrm{nF}$, $C_2 = 10.3\,\mathrm{nF}$, $r_0 = 1\,\mathrm{k\Omega}$, $V_{\mathrm{dd}} = 5\,\mathrm{V}$, and $V_{\mathrm{bias}} = 1.5\,\mathrm{V}$). A 4-bit M-sequence circuit was constructed using D-FF IC (HD14174BP) and Ex-OR IC (TC4030BP), and was operated at $20\,\mathrm{kHz}$ frequency. We used nMOSFET (2SK1398) and pMOSFET (2SJ184) for the transconductance amplifier, and used inverter ICs (TC4069BP) for the buffer circuit. In our experiments, we constructed one oscillator only, and measured it several times (total trial run: N) instead of constructing multiple oscillators and measuring them simultaneously. This is because device mismatches among the oscillators would strongly affect the experimental results, and here we wanted to control these effects.

We first examined single oscillator's properties ($N = 1$). Figure 6(a) shows the time courses of u_i and v_i of the oscillator circuit. We observed fluctuations in u_i
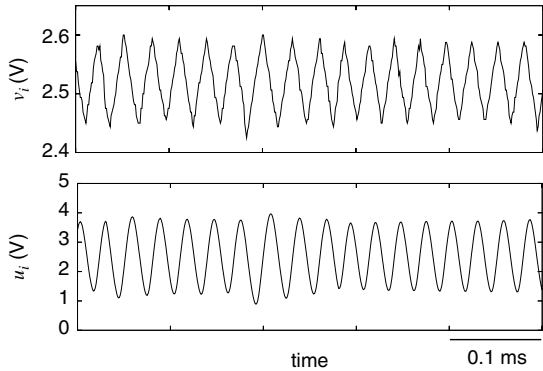
(a)
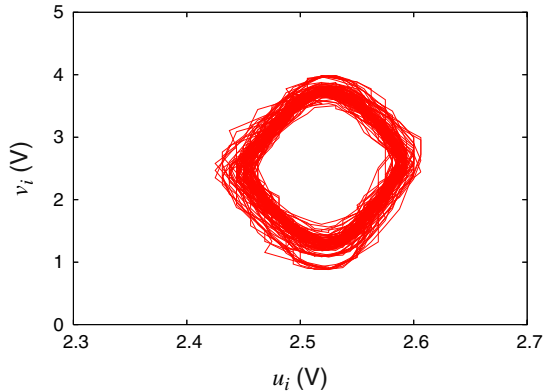
(b)

Fig. 6. Experimental results of single oscillator circuit: (a) time courses of u_i and v_i and (b) trajectories of u_i and v_i of noisy oscillator.

and v_i due to common random impulses produced by the M-sequence generator. Figure 6(b) shows trajectories of u_i and v_i of the measured oscillator. We confirmed the limit-cycle oscillations, and confirmed that the trajectories were clearly fluctuated around the limit-cycle orbit.

Next we observed population activities of multiple oscillators ($N = 10$: 10 trials with the single oscillator). We applied the same initial conditions for each trial when no random impulses were applied, while we applied different initial conditions when common random impulses were applied. Figures 7(a) and 7(b) show raster plots where vertical bar were plotted at $v_i > V_{\mathrm{dd}}/2$ and $dv_i/dt > 0$. When no random impulses were applied to the oscillators, their phases were not uniform because no interaction occurred among the oscillators [Fig. 7(a)]. However, when random impulses were applied to all the oscillators, they exhibited phase synchronization
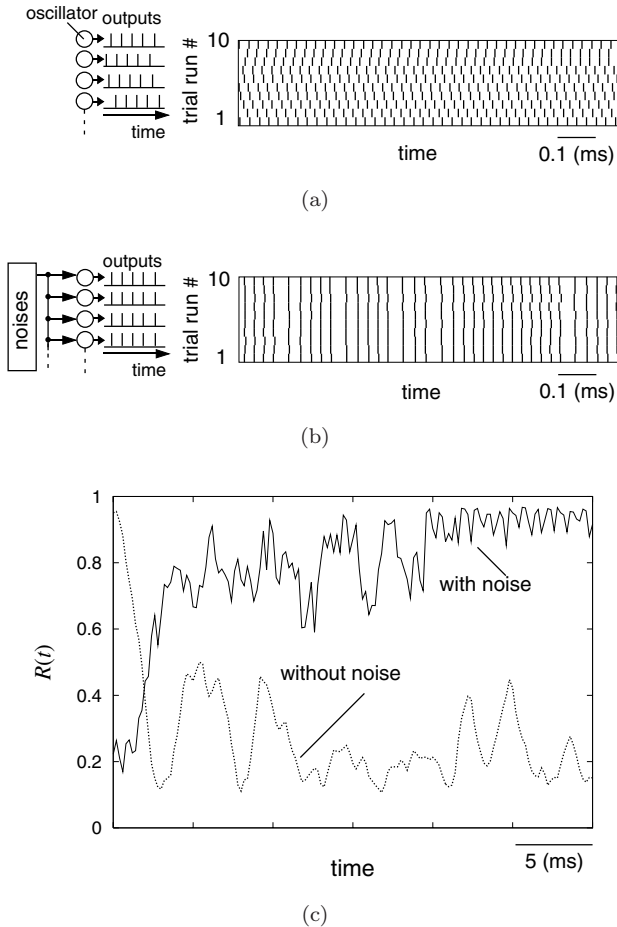

(a)

(b)

(c)

Fig. 7. Experimental results: (a) raster plots of 10 oscillators without random impulses, (b) raster plots of 10 oscillators with random impulses, and (c) time course of order parameters.

although they did not have any interaction [Fig. 7(b)] as shown in Sec. 2. When all
the oscillators are identical and environmental noise is small enough, the phase dif-
ferences among the oscillators that receive common random impulses approach 0.
Figure 7(c) shows the time course of the $R(t)$ without random impulses (dotted
line) and with random impulses (solid line). $R(t)$ was almost 1 when $t = 0$, but
$R(t)$ immediately deceased as t increased and stayed at a low value when random
impulses were not given. This means that time-dependent small (but unavoidable)
environmental noises led to the desynchronization. When random impulses were
applied, phases of the oscillators were almost random at $t = 0$, so $R(t)$ was around 0.
Then $R(t)$ gradually approached to 1 at 25–30 ms. This demonstrated that phase
synchronization among the individual oscillators was stochastically induced by ran-
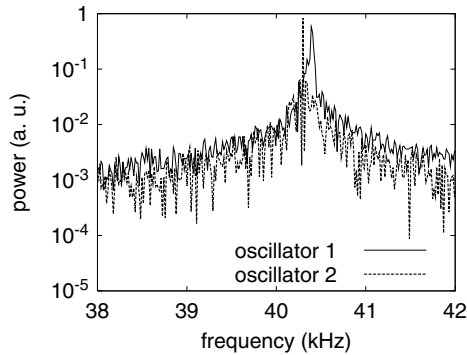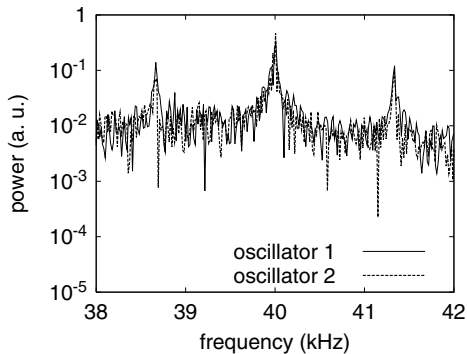dom impulses.
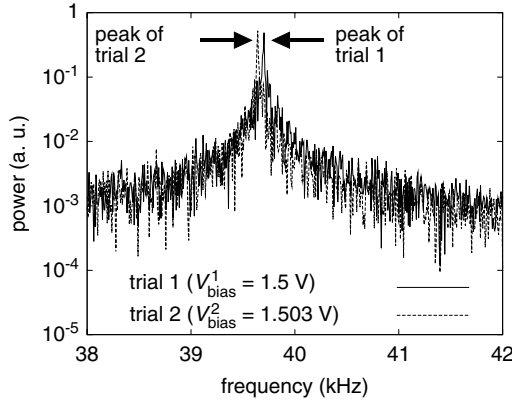
(a)
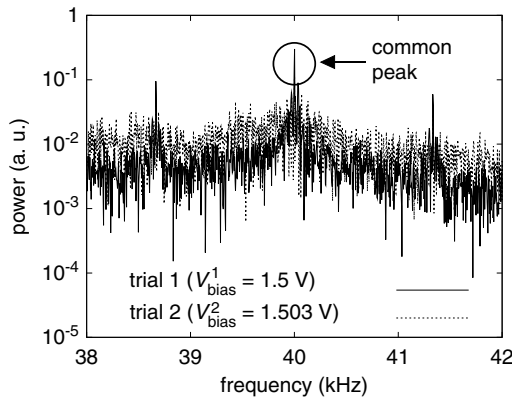
(b)

Fig. 8. Power spectrum for different trials: (a) without random impulses and (b) with random
impulses.

Next, we examined the effects of device mismatches on the phase synchronization. Although the results shown in Fig. 7 demonstrated that the oscillators were synchronized by random impulses, the variation in circuit characteristics would not be negligible in practical situations. We mimicked these effects in the way described in our previous work [8]; i.e., V_{bias} which determines the oscillators' intrinsic frequency was distributed as the most significant parameter. We compared the results between two trials ($N = 2$). In the first trial, we measured a circuit with bias condition $V_{\text{bias}}^1 = 1.5\,\text{V}$. At the second trial, we measured the circuit with $V_{\text{bias}}^2 = V_{\text{bias}}^1 - 3\,\text{mV}$. Figure 8 shows the power spectrums of the oscillator outputs (v_i). When no random impulses were applied [Fig. 8(a)], each oscillator had a different peak frequency because their intrinsic frequencies were governed by V_{bias}^1 and V_{bias}^2. However, when random impulses were applied [Fig. 8(b)], the oscillators in both trials had the same peak frequency, although their intrinsic frequencies were different. This indicates that even if small transistor mismatch occurs in the oscillator circuits, their phases would be synchronized by applying common random impulses.

(a)

(b)

Fig. 9. Power spectrum of two nonidentical oscillators: (a) without random impulses and (b) with random impulses.
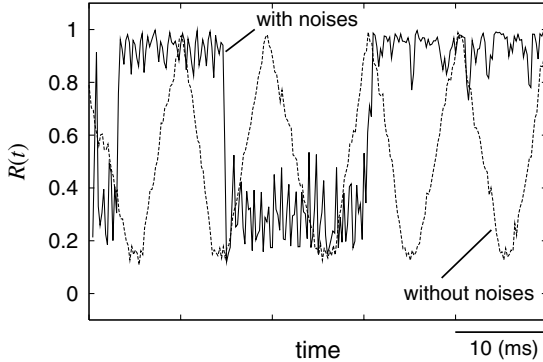
Fig. 10. Time courses of order parameter values for different oscillators.

Finally, we employed two real (nonidentical) oscillator circuits, and examined the effects of real device mismatches on the phase synchronization. Figure 9 shows the power spectrums of the two oscillators. When we applied common V_{bias} (1.47 V), fundamental frequencies of oscillator 1 and 2 were 40.4 kHz and 40.3 kHz, respectively, for given discrete devices [Fig. 9(a)]. When random impulses were applied [Fig. 9(b)], the oscillators had the same peak frequency, as expected in Fig. 8(b); i.e., random impulses forced the oscillators to have the same peak frequency. However, the results shown in both Figs. 8(b) and 9(b) do not ensure that random impulses certainly forced the phase synchronization among the nonidentical oscillators. Figure 10 shows time courses of order parameter values $R(t)$ under circuit conditions of Fig. 9. When no random impulses were applied, $R(t)$ was always lower than 1 [sometimes $R(t)$ approached to 1, but the value was suddenly decreased as shown in Fig. 10 (dashed line)]. In contrast, when random impulses were applied, two temporal states appeared; i.e., $R(t) \approx 1$ and $R(t) \ll 1$, and these states appeared in turn, as shown in Fig. 10 (solid line). This clearly showed that random impulses certainly forced phase synchronization among nonidentical oscillators for a short period, but the structure was broken by frequency mismatches for another short period.

5. Conclusion

We experimentally tested noise-induced synchronization among electrical oscillator circuits receiving common random impulses. The oscillators exhibited phase synchronization when they received random impulses, whereas they exhibited desynchronization when they did not received random impulses. Moreover, we experimentally showed that two oscillators having small difference in their intrinsic frequency had the same peak frequency in the power spectrum when they received common random impulses.

Acknowledgments

References

[1] C. Zhou and J. Kurths, Noise-induced phase synchronization and synchronization transitions in chaotic oscillators, *Phys. Rev. Lett.* **88** (2002) 230602.

[2] C. Zhou, J. Kurths, I. Z. Kiss and L. Hudson, Noise-enhanced phase synchronization of chaotic oscillators, *Phys. Rev. Lett.* **89** (2002) 014101.

[3] J. A. Freund, S. Barbay, S. Lepri, A. Zavatta and G. Giacomelli, Noise-induced phase synchronization: Theoretical and experimental results, *Fluct. Noise Lett.* **3** (2003) L195–L204.

[4] H. Nakao, K. Arai and K. Nagai, Synchrony of limit-cycle oscillators induced by random external impulses, *Phys. Rev. E* **72** (2005) 026220.

[5] H. Nakao, K. Arai and Y. Kawamura, Noise-induced synchronization and clustering in ensembles of uncoupled limit-cycle oscillators, *Phys. Rev. Lett.* **98** (2007) 184101.

[6] K. Arai and H. Nakao, Phase coherence in an ensemble of uncoupled limit-cycle oscillators receiving common Poisson impulses, *Phys. Rev. E* **77** (2007) 036218.

[7] H. R. Wilson and J. D. Cowan, Excitatory and inhibitory interactions in localized populations of model neurons, *Biophys. J.* **12** (1972) 1.

[8] A. Utagawa, T. Asai, T. Hirose and Y. Amemiya, Noise-induced synchronization among sub-RF CMOS analog oscillators for skew-free clock distribution, *IEICE Trans. Fundam. Electron. Commun. Comput. Sci.* **E91−A** (2008) 2475–2481.

[9] Y. Kuramoto, *Chemical Oscillation, Waves and Turbulence* (Springer-Verlag, Tokyo, 1984).

[10] T. Asai, Y. Kanazawa, T. Hirose and Y. Amemiya, Analog reaction-diffusion chip imitating the Belousov–Zhabotinsky reaction with hardware Oregonator model, *Int. J. Unconv. Comput.* **1** (2005) 123–147.

[11] G. M. Tovar, T. Asai, T. Hirose and Y. Amemiya, Critical temperature sensor based on oscillatory neuron models, *J. Signal Process.* **12** (2008) 17–24.

[12] M. Cohn and A. Lempel, On fast M-sequence transforms, *IEEE Trans. Inf. Theory* **IT-23** (1977) 135–137.